Brazilian Journal
of Chemical
Engineering

ISSN 0104-6632
Printed in Brazil
www.abeq.org.br/bjche

Vol. 29, No. 02, pp. 253 - 264, April - June, 2012

WALL EFFECTS ON THE CROSS-BUOYANCY AROUND A SQUARE CYLINDER IN THE STEADY REGIME

A. K. Dhiman*, N. Sharma and S. Kumar

Department of Chemical Engineering, Indian Institute of Technology Roorkee, 247 667, India.
*Assistant Professor, Department of Chemical Engineering, Indian Institute of Technology Roorkee, 247 667,
Phone: + 91-1332-285890 (O), + 91-9410329605 (M), India.
E-mail: dhimuamit@rediffmail.com; amitdfch@iitr.ernet.in

(Submitted: February 25, 2011 ; Revised: October 24, 2011 ; Accepted: October 31, 2011)

Abstract - The effects of blockage ratio on the combined free and forced convection from a long heated square obstacle confined in a horizontal channel are investigated in this work. The numerical computations are performed in the steady regime for Reynolds number = 1 – 30, Richardson number = 0 – 1 for blockage ratios of 0.125 and 0.25 for the fixed Prandtl number of 0.7 (air). The governing equations, along with appropriate boundary conditions, are solved by using a semi-explicit finite volume method implemented on the collocated grid arrangement. The total drag and lift coefficients, local and average Nusselt numbers and the representative streamline, vorticity and isotherm patterns are presented to elucidate the role of blockage ratio on the cross-buoyancy across a confined square cylinder. The asymmetry in the flow and temperature fields decreases with increasing value of the blockage ratio. Similar to forced convection, the total drag coefficient increases with increasing value of the blockage ratio for the fixed values of the Reynolds and Richardson numbers.
Keywords: Square obstacle; Cross-buoyancy; Blockage ratio; Drag; Lift; Nusselt number.

INTRODUCTION

The combined free and forced (or mixed) convection around obstacles of circular and/or square cross-sections at low Reynolds numbers has received considerable attention in recent years due to its fundamental and pragmatic relevance. These obstacles have a variety of engineering applications in compact heat exchange systems, oil and gas pipelines, flow metering devices and flow dividers, etc. The present work is concerned with the effects of wall confinement on the mixed convection across a long square cylinder confined in a channel under the influence of cross-buoyancy in the steady flow regime.

A wealth of information on the mixed convection around an unconfined obstacle of circular cross-section in both steady and unsteady flow regimes can be found elsewhere (Morgan, 1975; Zdravkovich, 1997, 2003; Farouk and Guceri, 1982; Ho *et al*., 1990; Singh *et al*., 1998; Biswas and Sarkar, 2009). Farouk and Guceri (1982) analyzed the two-dimensional steady mixed and free convections from an isothermal circular cylinder in a vertical channel with adiabatic walls for a fixed blockage ratio of 0.1667. Ho *et al*. (1990) investigated the buoyancy-aided convection heat transfer from a horizontal cylinder situated in a vertical adiabatic duct in the Reynolds number range $20 \le \mathrm{Re} \le 60$ and Richardson number up to 4. The average Nusselt number was found to be insensitive to the variation of either the position of the cylinder in the duct or the duct height. Singh *et al*. (1998) simulated the mixed convection from a heated/cooled circular cylinder for the range of values of the Richardson number $-1 \le \mathrm{Ri} \le 1$ in a

*To whom correspondence should be addressed

vertical channel ($\beta = 0.25$) for a fixed Reynolds number of 100 and Prandtl number of 0.7. They found the breakdown of the Karman vortex street at a Richardson number of about 0.15. Biswas and Sarkar (2009) examined the vortex shedding process behind a heated cylinder under the influence of thermal buoyancy at low Reynolds numbers ($Re = 10 - 45$) in cross-flow. The steady separated flows become unsteady (periodic) in the presence of superimposed thermal buoyancy.

In contrast, much less information is available on the mixed convection from a square obstacle confined in a channel. In the unsteady (periodic) cross-flow regime, Biswas *et al*. (1990) investigated the 2-D mixed convection across a horizontal square cylinder confined in the channel for varying values of Reynolds number and Grashof number for a fixed blockage ratio of 0.25. They reported that the periodicity of flow and asymmetry of the wake can occur at lower Reynolds numbers than that in pure forced convection. Turki *et al*. (2003) numerically investigated the 2-D unsteady mixed convection from a square cylinder (horizontal) for Reynolds number = 120 – 200 and Pr = 0.71, but for very low values of the Richardson number (i.e., $Ri = 0 - 0.1$) for a fixed blockage ratio of 0.25. The value of the critical Reynolds number (i.e., onset of periodic flow) decreases, while the Strouhal number increases with increasing Richardson number. They also proposed Nusselt number correlations for different values of the Richardson number (Ri = 0, 0.05 and 0.1).

Sharma and Eswaran (2005) investigated the effects of aiding/opposing buoyancy (Ri = -1 to 1) and blockage ratio (0.1, 0.3 and 0.5) on the flow and heat transfer from an isothermal square cylinder for the fixed values of the Reynolds number of 100 and Prandtl number of 0.7. The Strouhal number and the Nusselt number were found to increase with increasing Richardson number and increasing blockage ratio in the unsteady regime. Perng and Wu (2007) studied the effects of aiding/opposing buoyancy on the turbulent flow field and heat transfer across a square cylinder in the vertical channel for the range of conditions: Ri = -1 to 1, $\beta = 0.1, 0.3, 0.5$, $Pr = 0.71$ and $Re = 5000$.

On the other hand, in the steady cross-flow regime, Dhiman *et al*. (2008a) examined the mixed convection, (Re = 1 – 30, Ri = 0 – 1) across a long confined square cylinder for varying values of Prandtl number (0.7 - 100) for a fixed value of the blockage ratio of 0.125. The influence of the Richardson number on the total drag coefficient and the average Nusselt number is found to be qualitatively similar to the unconfined mixed convection case. In the unbounded steady flow regime, excellent information on the laminar mixed convection flow and heat transfer to Newtonian and non-Newtonian power-law fluids from a heated square cylinder under the influence of cross-buoyancy is reported elsewhere (Dhiman *et al*., 2007).

In summary, Sharma and Eswaran (2005) investigated the effects of blockage ratio for aiding/opposing buoyancy around a confined square cylinder for a fixed value of the Reynolds number of 100 in the unsteady laminar flow regime. In the turbulent flow regime, Perng and Wu (2007) investigated the effects of blockage ratio in aiding/opposing buoyancy around a confined square cylinder for a fixed value of the Reynolds number of 5000. Dhiman *et al*. (2008a) examined the steady mixed convection across a long confined square cylinder for a fixed blockage ratio of 0.125. Thus, as far as known to us, no numerical/experimental study is available on the cross-buoyancy around a long square obstacle at different values of blockage ratios in the steady confined flow regime. Therefore, one of the objectives of this study is to investigate the effects of wall confinement on the mixed convection from a square cylinder in the steady flow regime. The other objective is to investigate the onset of flow separation at different values of the Reynolds number, Richardson number and blockage ratio. A variety of engineering parameters such as total drag and lift coefficients, local and average Nusselt numbers and the representative streamline, vorticity and isotherm contours are presented in order to examine the effects of blockage ratio around a square obstacle in the steady cross-buoyancy regime.

PROBLEM STATEMENT, GOVERNING EQUATIONS AND BOUNDARY CONDITIONS

An incompressible, 2-D steady flow is flowing from left to right over a long (heated) square obstacle confined in a horizontal channel. Figure 1 presents the schematics of the flow around a long square obstacle. This cylinder of square cross-section is exposed to a parabolic velocity field with maximum velocity U_{max} at a uniform temperature, T_∞, at the inlet. The obstacle is located in the middle at an upstream dimensionless distance of X_u / b from the inlet and at a downstream dimensionless distance of X_d / b from the outlet. The total dimensionless length of the computational domain is L_1 / b in the axial direction; however, the dimensionless height of the computational domain

is L_2 / b in the lateral direction. The upstream and the downstream distances used here are 8.5 b and 16.5 b, respectively (Dhiman *et al*., 2008a).

The dimensionless continuity, x- and y-components of Navier-Stokes equations and the thermal energy equation (assuming negligible dissipation and constant thermo-physical properties except for the body force term in the momentum equation (Boussinesq approximation)) are given by Eqs. (1) – (4).

Continuity equation

$$\frac{\partial U}{\partial x}+\frac{\partial V}{\partial y}=0 \tag{1}$$

x-component

$$\frac{\partial U}{\partial t}+\frac{\partial (UU)}{\partial x}+\frac{\partial (VU)}{\partial y}=-\frac{\partial p}{\partial x}+\frac{1}{Re}\left(\frac{\partial^2 U}{\partial x^2}+\frac{\partial^2 U}{\partial y^2}\right) \tag{2}$$

y-component

$$\frac{\partial V}{\partial t}+\frac{\partial (UV)}{\partial x}+\frac{\partial (VV)}{\partial y}= -\frac{\partial p}{\partial y}+\frac{1}{Re}\left(\frac{\partial^2 V}{\partial x^2}+\frac{\partial^2 V}{\partial y^2}\right)+RiT \tag{3}$$

Energy equation

$$\frac{\partial T}{\partial t}+\frac{\partial (UT)}{\partial x}+\frac{\partial (VT)}{\partial y}=\frac{1}{Re\,Pr}\left(\frac{\partial^2 T}{\partial x^2}+\frac{\partial^2 T}{\partial y^2}\right) \tag{4}$$

In Equations (2) – (4), the three dimensionless parameters Re, Ri and Pr are defined as Reynolds number, $Re=\rho U_{max} b/\mu$, Richardson number, $Ri=Gr/Re^2$ and Prandtl number, $Pr=\mu c_p/k$, respectively.

The following boundary conditions may be written in their dimensionless form as (Figure 1).

- Inlet boundary condition: $U=4\beta y(1-\beta y)$ where $\beta=b/L_2$; $V=0$ and $T=0$.
- Upper and lower boundary conditions: $U=0$; $V=0$ and $\partial T/\partial y=0$.
- Boundary condition on the surface of the square obstacle: $U=0$; $V=0$ (no-slip) and $T=1$.
- Exit boundary condition: $\partial U/\partial x=0$, $\partial V/\partial x=0$ and $\partial T/\partial x=0$.

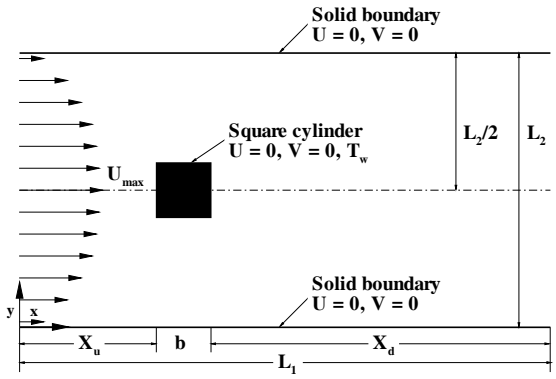

Figure 1: Schematics of the flow around a long confined square cylinder

NUMERICAL DETAILS

The details of the grid and the solution methodology used in this study can be found elsewhere (Dhiman *et al*., 2005, 2006, 2008a,b). The computational grid structure used here is generated by using MATLAB. The computational grid structure consists of five different zones with uniform and non-uniform grid distributions in both the x- and y-directions. The grid distribution is uniform with a constant cell size, $\Delta = 0.25$ b, in an outer region that extends beyond 4 b upstream and downstream of the cylinder in the x-direction. A fine grid size, $\delta = 0.01$ b, is clustered in an inner region near the cylinder over a distance of 1.5 b to adequately capture the wake dynamics in both the x- and y- directions. The hyperbolic tangent function has been used to stretch the cell sizes between the two limits of Δ and δ in the x-direction (Thompson *et al*., 1985). Also, a fine grid of size δ is clustered near the upper and lower walls of the channel to capture the wake-wall interactions adequately. An algebraic expression has been used to generate the mesh in the region of 0.25 b away from the cylinder and the channel walls in the y-direction (Hoffmann, 1989). The identical computational grid structure is used here for the two blockage ratios as reported elsewhere (Dhiman *et al*., 2005, 2008a,b).

In this work, an in-house semi-explicit finite volume method implemented on the collocated grid arrangement has been used to solve the governing equations, along with the appropriate boundary conditions in which momentum equations are discretized in an explicit manner, whereas the pressure gradient terms are treated implicitly (Dhiman *et al*., 2005, 2006, 2008a,b; Sharma and Eswaran, 2003).

RESULTS AND DISCUSSION

In this study, full-domain numerical calculations are performed for the range of conditions: Re = 1, 5, 10, 20, 30, Ri = 0, 0.25, 0.5, 1 and β = 0.125, 0.25 for a fixed Prandtl number of 0.7 (air) in the steady confined flow regime. The present study is restricted for the Prandtl number of 0.7 as the buoyancy effects decrease with increasing Prandtl number (Dhiman *et al*., 2007, 2008a). The values of the blockage ratios are chosen based upon information available in the literature (Biswas *et al*., 1990; Turki *et al*., 2003). Additional computations are also carried out in order to investigate the onset of flow separation at different values of the Reynolds number, Richardson number and blockage ratio. The detailed benchmarking of the present numerical solution procedure can be found in our earlier studies (Dhiman *et al*., 2005, 2008a,b).

The following subsections present the details about the engineering parameters such as drag and lift coefficients, local and average Nusselt numbers and the derived variables such as stream function and vorticity. The temperature field is presented by way of isotherm contours for different values of the Reynolds and Richardson numbers and blockage ratio.

Flow Patterns

The detailed flow patterns in the vicinity of the long square cylinder are presented by streamline and vorticity contours. Figures 2 (a - l) and 3 (a - l) present the streamline contours for Reynolds numbers of 1, 10, 20 and 30 for the blockage ratios of 0.25 and 0.125 for the fixed Prandtl number of 0.7 at different values of the Richardson number (Ri = 0.25, 0.5 and 1). The vorticity profiles are shown in Figures 4 (a - l) and 5 (a - l) at different values of Reynolds and Richardson numbers and blockage ratios. The extensive details on the confined flow and heat transfer around a square cylinder for Ri = 0 (forced convection) in the steady regime can be found elsewhere (Dhiman *et al*., 2005, 2008b). The flow is found to be symmetric for the value of the Richardson number of zero for all the values of the Reynolds number at the different values of the blockage ratios considered in this work. No flow separation is found at Re = 1 for Ri = 0 – 1 for the blockage ratios of 0.25 and 0.125. However, the flow separation is found to occur at Re = 2 at different values of the Reynolds number, Richardson number and blockage ratio. Thus, the onset of flow separation exists between Re = 1 and 2 for the range of conditions studied here.

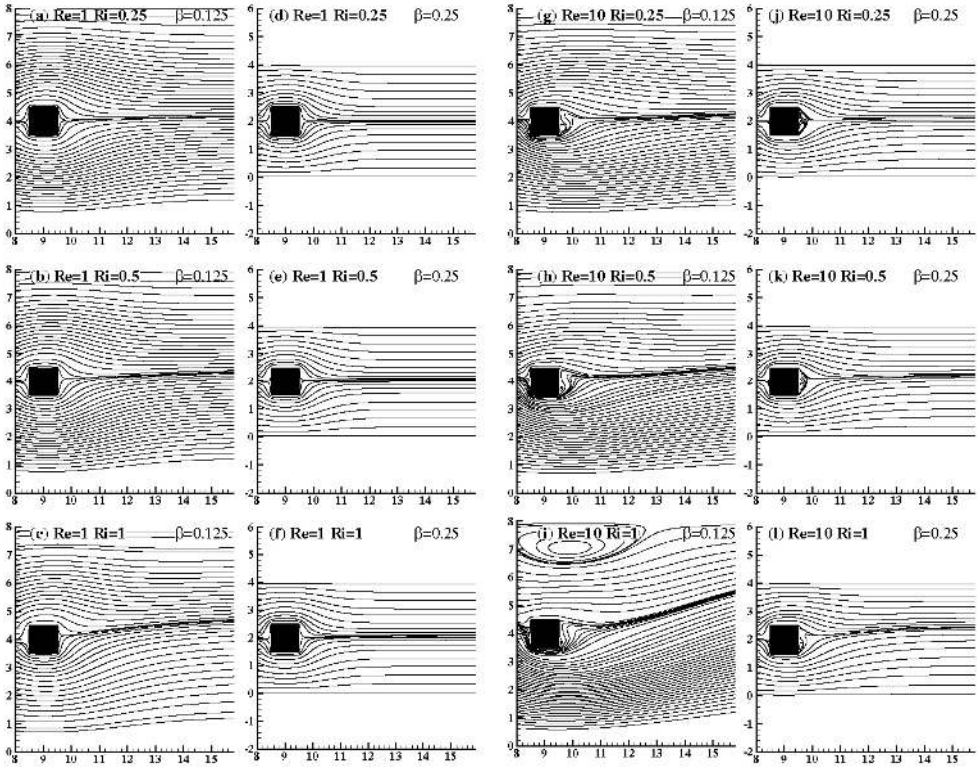

Figure 2: Streamline profiles for Re = 1 and 10 for Ri = 0.25, 0.5 and 1 at different blockage ratios

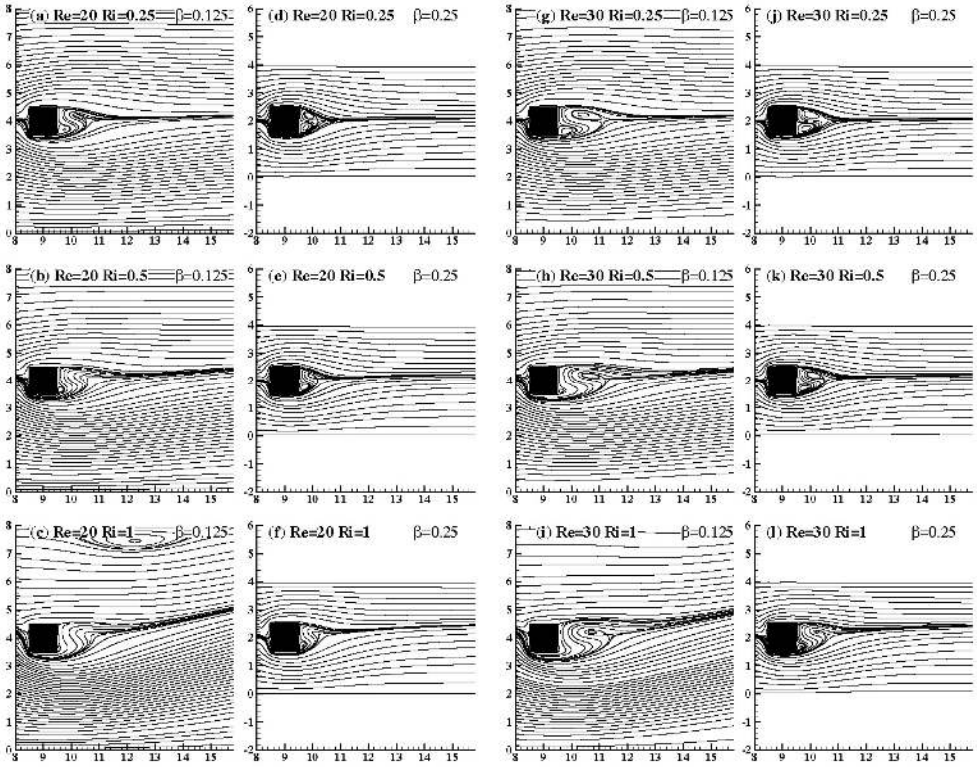

Figure 3: Streamline profiles for $\mathrm{Re} = 20$ and 30 for $\mathrm{Ri} = 0.25$, 0.5 and 1 at different blockage ratios

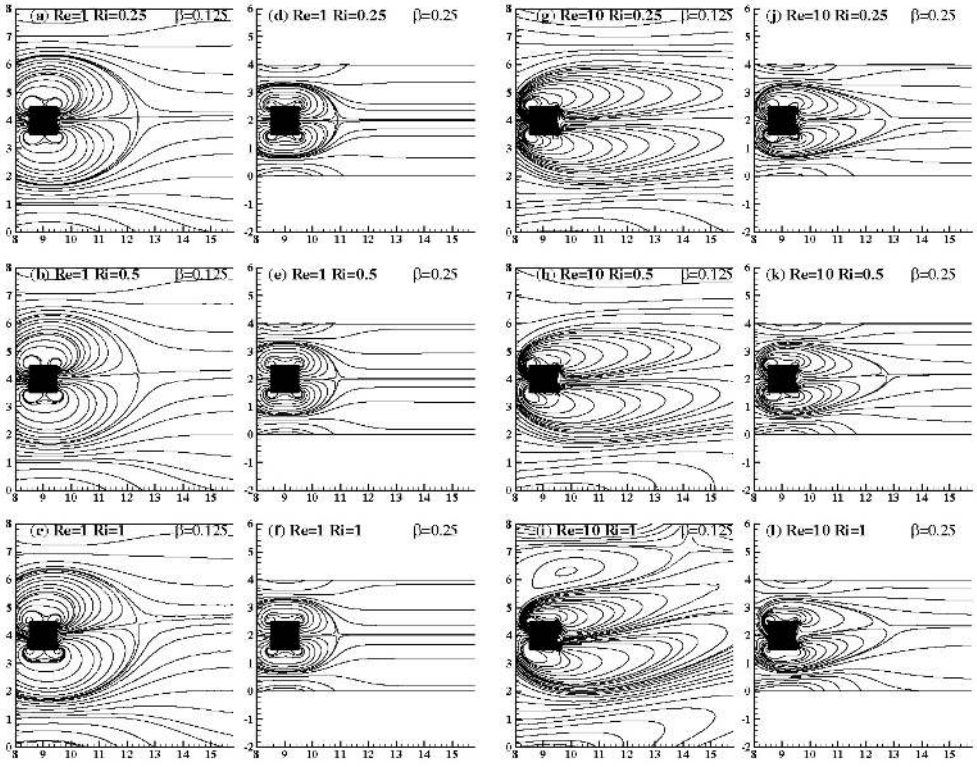

Figure 4: Vorticity profiles for $\mathrm{Re} = 1$ and 10 for $\mathrm{Ri} = 0.25$, 0.5 and 1 at different blockage ratios

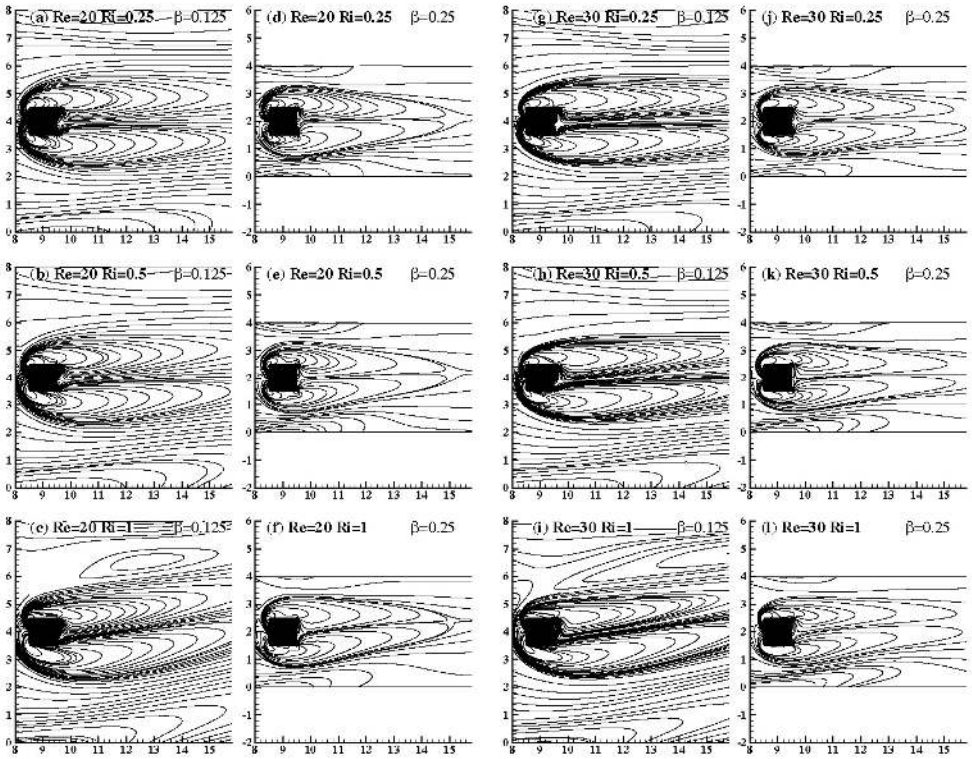

Figure 5: Vorticity profiles for $\mathrm{Re} = 20$ and 30 for $\mathrm{Ri} = 0.25$, 0.5 and 1 at different blockage ratios

As the value of the Reynolds number gradually increases ($\mathrm{Re} > 1$), two symmetric vortices are formed behind the square cylinder for $\mathrm{Ri} = 0$ and the size of these vortices increases as well. Note that, irrespective of the values of the Richardson number and the blockage ratios, no wake (i.e., closed near vortex) is formed behind the square obstacle for the Reynolds number of unity. On the other hand, flow symmetry is lost with the introduction of the cross-buoyancy and as the value of the Richardson number gradually increases (i.e., $\mathrm{Ri} > 0$), the degree of asymmetry increases at different values of blockage ratios. Interestingly, these effects are found to be more pronounced for the low value of the blockage ratio, e.g., $\beta = 0.125$ in this study. This is due to the fact that the flow tends to stabilize with increasing value of the blockage ratio. Further, as the value of the Reynolds number gradually increases ($\mathrm{Re} > 1$), wakes formed in the rear of the square cylinder lose symmetry due to the higher mass flow rate below the square obstacle than that above it. It is also clear from these figures (Figures 2g - l to 3 and 4g - l to 5) that the size of the wake region behind the square cylinder (i.e., near the bottom-rear corner of the cylinder) decreases with increasing value of the Richardson number for the blockage ratio of 0.25; however, the wake gradually diminishes as the Richardson number increases for the blockage ratio of 0.125. In addition, a wake region is also observed on the top wall of the channel for the Reynolds numbers of 10 and 20 for $\mathrm{Ri} = 1$ and $\beta = 0.125$ (Figures 2i, 3c, 4i and 5c). This is due to the flow reversal at the top channel wall due to the higher mass flow rate below the square cylinder than above it (Figures 2i, 3c, 4i and 5c). On the other hand, as the value of the blockage ratio increases from 0.125 to 0.25, the buoyancy effects decrease and no flow reversal is observed for the blockage ratio of 0.25 for the range of conditions studied here. Furthermore, the vorticity contours can also be used to locate the separation points and to investigate the behavior of the fluid flow, especially near the channel walls (Figures 4 and 5).

Isotherm Patterns

The temperature fields around the square obstacle are represented by isotherm profiles in Figures 6 (a - l) and 7 (a - l) for $\mathrm{Re} = 1 - 30$, $\mathrm{Ri} = 0.25 - 1$ and $\beta = 0.125,\ 0.25$ for the fixed value of the Prandtl number of 0.7. Similar to flow fields, asymmetry in temperature fields is observed here with the introduction of the cross-buoyancy for the different values of the blockage ratios (Figures 6 and 7).

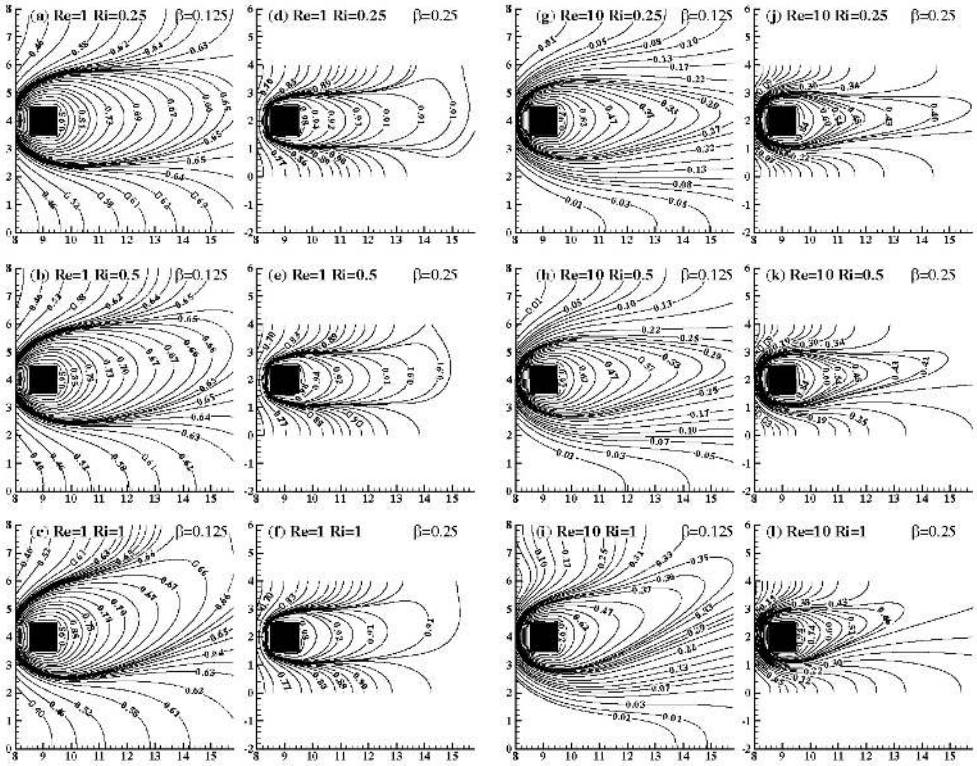

Figure 6: Isotherms for $\mathrm{Re} = 1$ and 10 for $\mathrm{Ri} = 0.25$, 0.5 and 1 at different blockage ratios

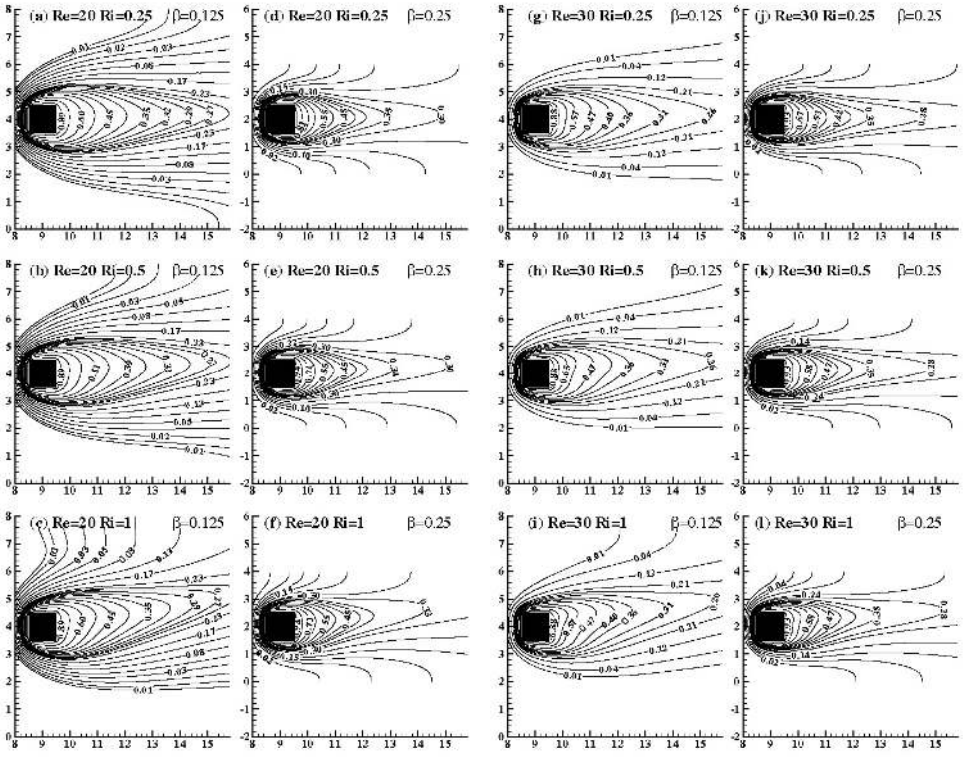

Figure 7: Isotherms for $\mathrm{Re} = 20$ and 30 for $\mathrm{Ri} = 0.25$, 0.5 and 1 at different blockage ratios

Further, an increase in the asymmetry of the temperature fields can also be seen as the value of Richardson number increases for the fixed values of Reynolds number and blockage ratio. However, these effects are observed to be more pronounced as the value of the blockage ratio decreases. The maximum crowding of isotherms on the front surface of the square cylinder can also be seen in these figures as compared to other surfaces of the square obstacle. This results in a higher value of the Nusselt number for the cylinder front surface than for the other surfaces of the square obstacle.

Drag Coefficient

The effects of blockage ratio, Reynolds and Richardson numbers on the total drag coefficient are presented in Figure 8 (a) in the steady regime. Similar to the forced convection case ($Ri = 0$), the total drag coefficient increases with increasing value of the blockage ratio for the fixed values of Reynolds and Richardson numbers. For instance, the maximum relative changes in the overall drag coefficient for the blockage ratio of 0.125 are found to be about 55.5%, 48.8%, 41.7%, 34.4% and 32.0% for $Re = 1$, 5, 10, 20 and 30 as compared to the total drag coefficient for the blockage ratio of 0.25. However, the slight change in the value of the drag is observed for the varying value of the Richardson number for the fixed values of blockage ratio and Reynolds number. The maximum relative changes in the values of the total drag coefficient, as compared to the forced convection case ($Ri = 0$), are found to be about 0.4% (at $Re = 5$), 1.7% (at $Re = 5$) and 10.6% (at $Re = 10$) for the Richardson numbers of 0.25, 0.50 and 1 for the blockage ratio of 0.125, respectively. However, the corresponding maximum changes in the values of total drag coefficient for the blockage ratio of 0.25 are found to be about 0.3%, 1.3% and 5.3% for the Richardson numbers of 0.25, 0.50 and 1 for the Reynolds number of 30, respectively. These results are also in line with the mixed convection around a horizontal square cylinder in the unconfined steady flow regime (Dhiman *et al*., 2007).

Lift Coefficient

Figure 8 (b) presents the variation of the total lift coefficient at different values of the Reynolds and Richardson numbers and blockage ratios. Due to the asymmetry in the steady flow field under the influence of cross-buoyancy, which gives rise to unbalanced shearing and pressure forces, non-zero values of the lift coefficient are obtained for the Richardson number range $0 < Ri \leq 1$ for the different values of the blockage ratios. Similar to unconfined mixed convection (Dhiman *et al*., 2007), the lift coefficient is found to be more sensitive than the drag coefficient for the range of conditions studied here. The total lift coefficient decreases with increasing value of the Richardson number for the fixed value of the Reynolds number (except $Re = 1$, where the lift coefficient increases with Richardson number) for the blockage ratio of 0.125. However, for the blockage ratio of 0.25, the total lift coefficient decreases with increasing value of the Richardson number for the fixed Reynolds number for the range Re = 1 – 30. As the value of the blockage ratio increases, the overall lift coefficient increases for the fixed values of Reynolds and Richardson numbers (except $Re = 1$). The lift coefficient decreases with increasing blockage ratio for the Reynolds number of unity. This is probably due to the fact that no flow separation occurs from the surface of the square cylinder for the Reynolds number of unity for the blockage ratios of 0.125 and 0.25.

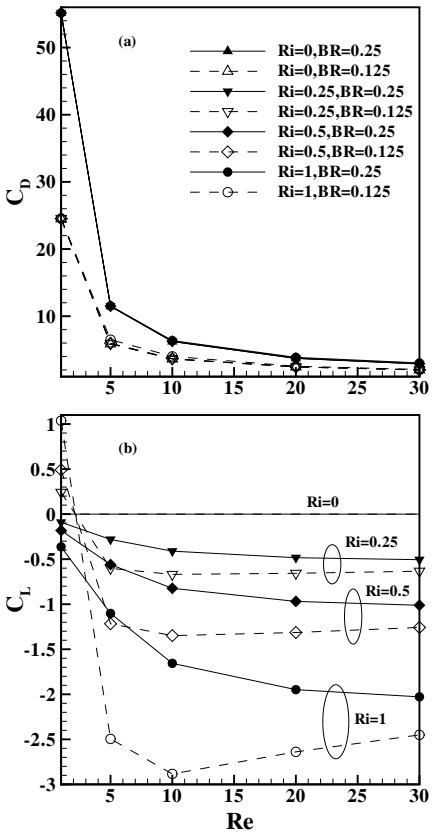

Figure 8: Variations of (a) mean drag coefficient and (b) mean lift coefficient with Reynolds number at different Richardson numbers and blockage ratios

Local and Average Nusselt Numbers

Figure 9 presents the variation of the local Nusselt number along the four surfaces of the 2-D square cylinder for the different values of the Reynolds number, Richardson number and blockage ratio for the fixed value of the Prandtl number of 0.7. This figure also includes the corresponding enlarged views for blockage ratios of 0.125 (Figures a1 – c1) and of 0.25 (Figures d1 – f1). In this study, the local Nusselt number is defined as $-\partial T/\partial n$, where n is the cylinder surface normal direction. With an increase in the value of the blockage ratio from 0.125 to 0.25, the value of the local Nusselt number decreases for the Reynolds number of unity for the fixed value of the Richardson number. The value of the local Nusselt number increases with increasing value of the blockage ratio in the range $1 < Re \leq 30$ for the fixed value of the Richardson number, but the value of the local Nusselt number decreases for $Re > 1$ and $Ri = 1$ from just before the top-front corner to the top-rear corner of the square cylinder. This is due to the higher mass flow rate below the square cylinder than above it.

The maximum enhancement in the values of the local Nusselt number with respect to the forced convection case ($Ri = 0$) are found to be about 10.8%, 12.3% and 26.3% for Reynolds numbers of 1, 20 and 30 for a Richardson number of unity and blockage ratio of 0.125, respectively. However, the corresponding maximum relative enhancement is found to be about 2.8%, 13.2% and 14.6% for the blockage ratio of 0.25, respectively.

The average Nusselt number is obtained here by averaging the local Nusselt number over the cylinder surfaces. The variation of the cylinder average Nusselt number is shown in Figure 10 for the two values of the blockage ratios at various values of the Reynolds and Richardson numbers. Similar to unconfined mixed convection (Dhiman *et al*., 2007), a slight variation in the value of the average Nusselt number can be seen for the fixed value of the blockage ratio, Reynolds and Richardson numbers (Figure 10).

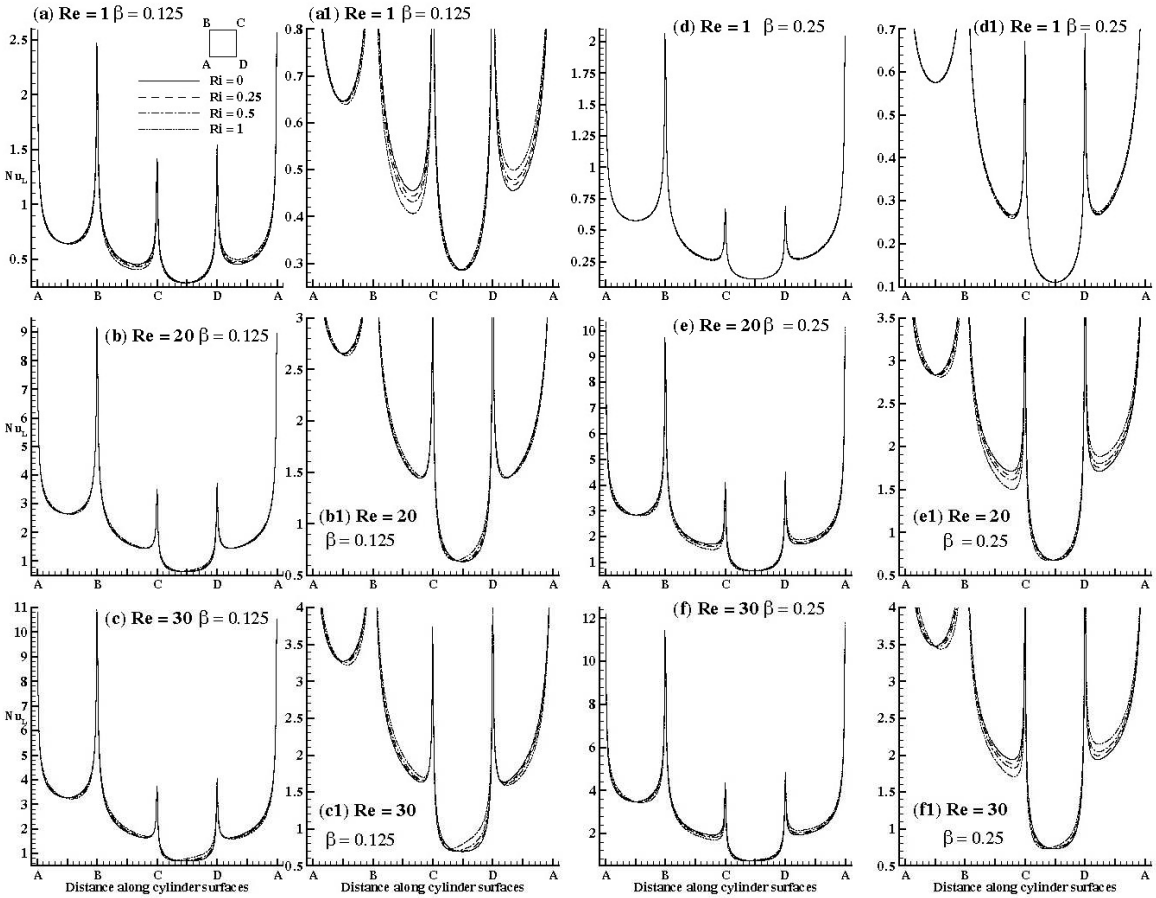

Figure 9: Variation of the local Nusselt number at different Reynolds and Richardson numbers and blockage ratios

The maximum enhancement in the value of the average Nusselt number is found to be about 2.7% as compared to the forced convection case for the Reynolds number of 5 and the Richardson number of unity for the blockage ratio of 0.125. However, for the blockage ratio of 0.25, the maximum gain in the average Nusselt number is found to be about 1.1% for the Reynolds number of 5 and the Richardson number of unity. Similar to the forced convection case, the average Nusselt number increases as the value of blockage ratio increases (except for the Reynolds number of unity) for the fixed value of the Reynolds number and the Richardson number. For $\mathrm{Re} = 1$, the average Nusselt number decreases with increasing value of the blockage ratio (Figure 10). This is due to the fact that no wake (or no closed near vortex) is formed behind the square cylinder for the Reynolds number of unity for the blockage ratios of 0.125 and 0.25. As the value of the blockage ratio is increased from 0.125 to 0.25, the maximum relative changes in the cylinder average Nusselt number are found to be about 42.9% (at $\mathrm{Ri} = 0$), 7.8% (at $\mathrm{Ri} = 1$), 10.0% (at $\mathrm{Ri} = 0$), 9.0% (at $\mathrm{Ri} = 0$) and 8.3% (at $\mathrm{Ri} = 0$) for the Reynolds numbers of 1, 5, 10, 20 and 30, respectively. Furthermore, the average Nusselt number of the front surface is found to be the highest, followed by the top/bottom surface and then the rear surface for the fixed values of the Reynolds number and the Richardson number for both the values of the blockage ratios.

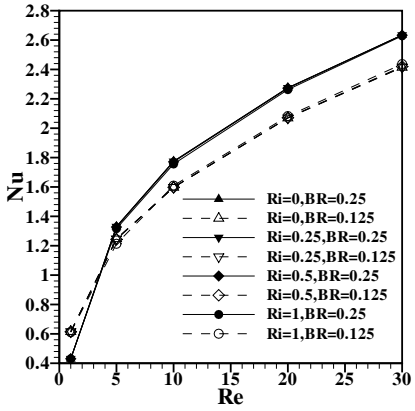

Figure 10: Variation of mean Nusselt number with Reynolds number at different Richardson numbers and blockage ratios

CONCLUSIONS

In this study, the effects of blockage ratio on the cross-buoyancy around a confined square cylinder in a channel are investigated for Reynolds number = 1 – 30, Richardson number = 0 – 1, blockage ratio = 0.125, 0.25 and Prandtl number = 0.7 in the 2-D steady flow regime. The flow field is represented by streamline and vorticity contours. However, the temperature field is represented by isotherm profiles in the vicinity of the long square cylinder. The engineering parameters such as total drag and lift coefficients and local and average Nusselt numbers are calculated for the above range of conditions. Similar to the forced convection case, the total drag coefficient increases with increasing value of the blockage ratio for the fixed values of Reynolds and Richardson numbers. The cylinder average Nusselt number is found to be insensitive to the variation of the values of the Richardson number for the fixed Reynolds number and the blockage ratio. As the value of the blockage ratio increases, the cylinder average Nusselt number increases, except for the Reynolds number of unity, for the range of conditions covered here.

NOMENCLATURE

b	side of the square obstacle	m
c_p	specific heat of the fluid	J kg^{-1} K^{-1}
C_D	drag coefficient $(= 2F_D / \rho U_{max}^2 b)$	
C_L	lift coefficient $(= 2F_L / \rho U_{max}^2 b)$	
F_D	drag force per unit length of the cylinder	N m^{-1}
F_L	lift force per unit length of the cylinder	N m^{-1}
g	gravitational acceleration	m s^{-2}
Gr	Grashof number $(= g\beta_V (T_w' - T_\infty)\rho^2 b^3 / \mu^2)$	
h	local heat transfer coefficient	W m^{-2} K^{-1}
$\overline{h}$	average heat transfer coefficient	W m^{-2} K^{-1}
k	thermal conductivity of the fluid	W m^{-1} K^{-1}
L_1	length of the computational domain	m
L_2	height of the computational domain	m
Nu	cylinder average Nusselt number $(= \overline{h} b / k)$	
Nu_L	local Nusselt number of the cylinder $(= hb / k)$	
p	pressure $(= p' / (\rho U_{max}^2))$	
Pr	Prandtl number $(= \mu c_p / k)$	
Re	Reynolds number $(= \rho U_{max} b / \mu)$	
Ri	Richardson number $(= \mathrm{Gr} / \mathrm{Re}^2)$	
t	time $(= t' / (b / U_{max}))$	

T	temperature $(= (T' - T_\infty) / (T'_w - T_\infty))$	
T_∞	temperature of the fluid at the inlet	K
T'_w	constant temperature at the surface of the cylinder	K
U	x- component of the velocity $(= U' / U_{max})$	
U_{max}	maximum velocity of the fluid at the inlet	m s^{-1}
V	y- component of the velocity $(= V' / U_{max})$	
x	stream-wise coordinate $(= x' / b)$	
X_d	downstream distance of the cylinder from the outlet	m
X_u	upstream distance of the cylinder from the inlet	m
y	transverse coordinate $(= y' / b)$	

Greek Symbols

β	blockage ratio $(= b / L_2)$	
β_V	coefficient of volumetric expansion	K^{-1}
μ	dynamic viscosity	Pa s
ρ	density of the fluid	kg m^{-3}

Subscripts

w	surface of the square cylinder

Superscript

'	dimensional variable

REFERENCES

Biswas, G., Laschefski, H., Mitra, N. K. and Fiebig, M., Numerical investigation of mixed convection heat transfer in a channel with a built-in square cylinder. Num. Heat Transfer, A, 18, 173-188 (1990).

Biswas, G. and Sarkar, S., Effect of thermal buoyancy on vortex shedding past a circular cylinder in cross-flow at low Reynolds numbers. Int. J. Heat Mass Transfer, 52, 1897-1912 (2009).

Dhiman, A. K., Chhabra, R. P. and Eswaran, V., Flow and heat transfer across a confined square cylinder in the steady flow regime: Effect of Peclet number. Int. J. Heat Mass Transfer, 48, 4598-4614 (2005).

Dhiman, A. K., Chhabra, R. P. and Eswaran, V., Effect of Peclet number on the heat transfer across a square cylinder in the steady confined channel flow regime. Proc. 18th National and 7th ISHMT-ASME Heat and Mass Transfer Conf., Indian Institute of Technology Guwahati, India (2006).

Dhiman, A. K., Anjaiah, N., Chhabra, R. P. and Eswaran, V., Mixed convection from a heated square cylinder to Newtonian and power-law fluids. Trans. ASME J. Fluids Eng., 129, 506-513 (2007).

Dhiman, A. K., Chhabra, R. P. and Eswaran, V., Steady mixed convection across a confined square cylinder. Int. Comm. Heat Mass Transfer, 35, 47-55 (2008a).

Dhiman, A. K., Chhabra, R. P. and Eswaran, V., Steady flow across a confined square cylinder: effects of power-law index and blockage ratio. J. Non-Newtonian Fluid Mech., 148, 141-150 (2008b).

Farouk, B. and Guceri, S. I., Natural and mixed convection heat transfer around a horizontal cylinder within confining walls. Num. Heat Transfer, A, 5, 329-341 (1982).

Ho, C. J., Wu, M. S. and Jou, J. B., Analysis of buoyancy-aided convection heat transfer from a horizontal cylinder in a vertical duct at low Reynolds number. Warme-und Stoffubertragung, 25, 337-343 (1990).

Hoffmann, K. A., Computational fluid dynamics for engineers. Engineering Education System, Austin, TX (1989).

Morgan, V. T., The overall convective heat transfer from smooth circular cylinders. Adv. Heat Transfer, 11, 199-264 (1975).

Perng, S. -W. and Wu, H. -W., Buoyancy-aided/ opposed convection heat transfer for unsteady turbulent flow across a square cylinder in a vertical channel. Int. J. Heat Mass Transfer, 50, 3701-3717 (2007).

Sharma, A. and Eswaran, V., A finite volume method. In: K. Muralidhar, T. Sundararajan (Eds.), Computational Fluid Flow and Heat Transfer, Narosa Publishing House, New Delhi, pp. 445-482 (2003).

Sharma, A. and Eswaran, V., Effect of channel-confinement and aiding/opposing buoyancy on the two-dimensional laminar flow and heat transfer across a square cylinder. Int. J. Heat Mass Transfer, 48, 5310-5322 (2005).

Singh, S., Biswas, G. and Mukhopadhyay, A., Effect of thermal buoyancy on the flow through a

vertical channel with a built-in circular cylinder. Num. Heat Transfer, A, 34, 769-789 (1998).

Thompson, J. F., Warsi, Z. U. A. and Mastin, C. W., Numerical grid generation: foundations and applications. Elsevier Science, New York, pp. 305-310 (1985).

Turki, S., Abbassi, H. and Nasrallah, S. B., Two-dimensional laminar fluid flow and heat transfer in a channel with a built-in heated square cylinder. Int. J. Thermal Sci., 42**,** 1105-1113 (2003).

Zdravkovich, M. M., Flow Around Circular Cylinders. Fundamentals, vol. 1, Oxford University Press, New York (1997).

Zdravkovich, M. M., Flow Around Circular Cylinders. Applications, vol. 2, Oxford University Press, New York (2003).